UM-PE11 Manual

LED and Laser Diode

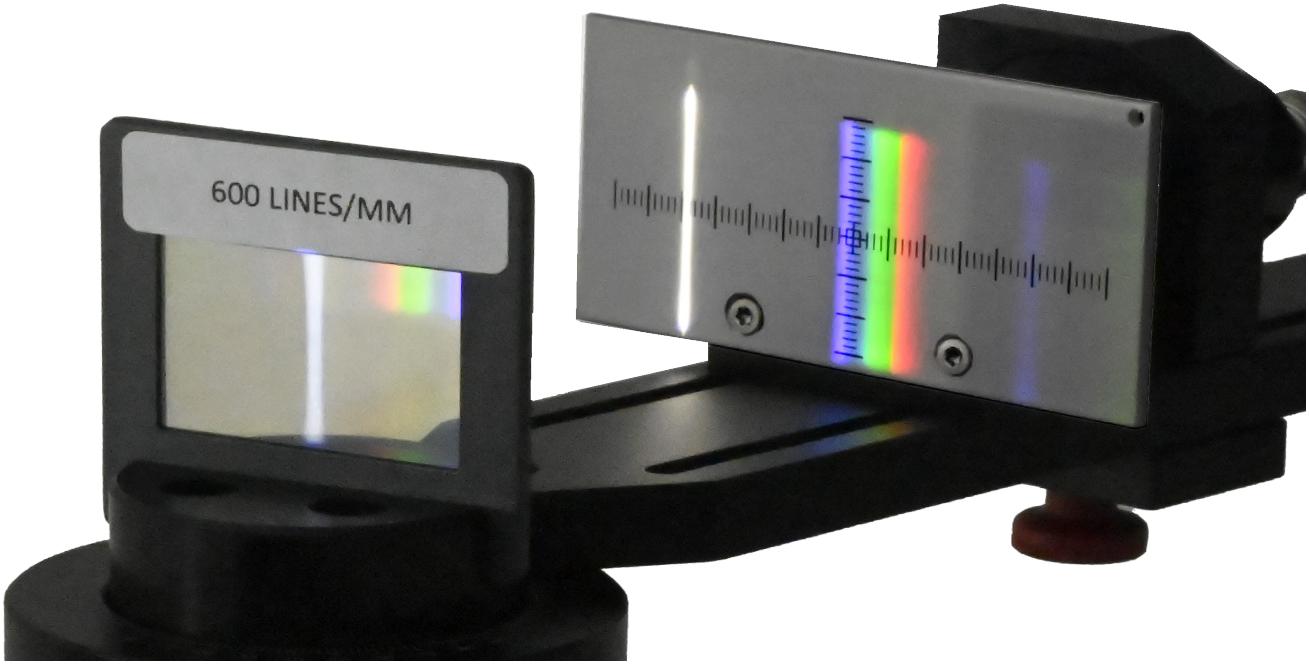

Table of Contents
Introduction
theory
Experimental setup
Measurements

Table of Content

1 Introduction

1.1 Laser diodes

The laser diodes are a special class of lasers. They differ from „conventional“ lasers in two points:

1. For the classical lasers the laser-active atoms (molecules or ions) are independent of one another and only the same energy levels are used for the laser process. This means in principle that in order to produce a population inversion an infinite number of atoms can contribute (Boltzmann statistics).

2. This is not the case with semiconductor lasers. Here a defined energy level can only be occupied by two active particles (electrons, Pauli principle). But in semiconductors, the wave functions of the individual atoms overlap to form a common energy band and the extent to which the level is occupied follows the Fermi Dirac statistics. When considering the laser process, the transition between the distribution of population in two energy bands instead of two energy levels must be taken into account as for conventional lasers.

Laser diodes do not have any inherently defined emission wavelength, because there are no two discrete energy levels that are responsible for the laser process as with traditional lasers, but rather an energy distribution of electrons in energy bands. The second important difference concerns the propagation of the laser light within the pn zone. The spatial intensity distribution of the laser beam is defined by the laser medium and not by the resonator as for normal lasers. The goal of this experiment is also the understanding and checking of the basic facts. Therefore the difference between a laser with two discrete energy levels and the semiconductor laser with the typical band structure will be discussed in the following.

1.2 The energy band model

Atoms or molecules at large distance (compared to the spatial dimensions) to their neighbors do not notice mutually their existence. They can be considered as independent particles. Their energy levels are not influenced by the neighboring particles.

The behavior will be different when the atoms are approached as it is the case within a solid body. Depending on the type of atoms and their mutual interaction the energy states of the electrons can change in a way that they even can abandon „their“ nucleus and move nearly freely within the atomic structure. They are not completely free, otherwise they could leave the atomic structure.
How the „free“ electrons behave and how they are organized will be the subject of the following considerations. From the fundamentals of electrostatics we know that unequal charges attract. Therefore it is easy to imagine that an atomic structure is formed by electrostatic forces.
In the following we will call it „crystal“. However, this model will fail latest when we try to justify the existence of solid Argon just by freezing it sufficiently. Since there is obviously some sort of binding within the crystal structure in spite of the fact that inert gases are neutral there must be additional forces which are responsible for this binding.

To understand these forces we must call on quantum mechanics for help. At the beginning this may be at bit difficult but it simplifies the later understanding. The Hamilton operator and Schroedinger's equation are supposed to be known. But the acceptance of the result of the following expertise on exchange interaction, exchange energy and tunnel effect for the formation of energy bands will be sufficient for further understanding provided quantum mechanics is considered as the background of all.

1.3 The binding of the hydrogen molecule

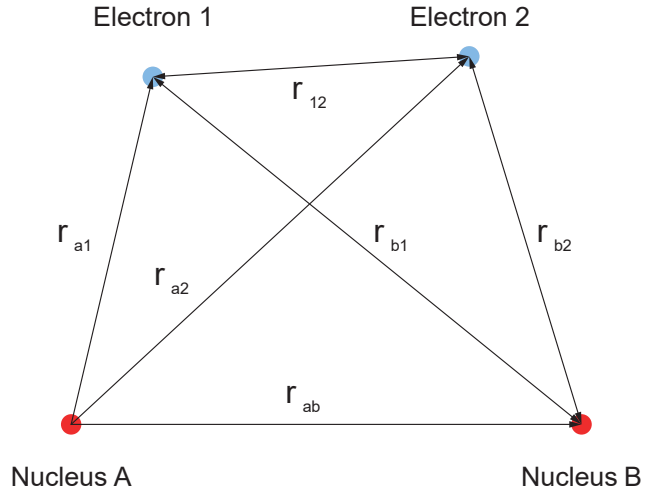

Fig. 1: Interaction of two hydrogen molecules

The total electric potential energy is:

$$U = -e^2 \cdot \left(\frac{1}{r_{a1}} + \frac{1}{r_{b2}} + \frac{1}{r_{b1}} + \frac{1}{r_{a2}} - \frac{1}{r_{ab}} \right) \qquad \textbf{(1)}$$

The following Schroedinger equation has to be solved:

$$\Delta\Psi_1 + \Delta\Psi_2 + 8\pi^2 \frac{m}{h^2} \cdot (E - U) \cdot \Psi = 0$$

For two hydrogen atoms without interaction the total energy will be

$$E = E_0(1) + E_0(2) = 2E_0$$

Correspondingly the eigenfunction ψ is the product of the eigenfunctions of the individual electrons belonging to the nuclei a and b.

$$\Psi_{12} = \Psi_a(1) \cdot \Psi_b(2)$$

Since we cannot distinguish between the individual electrons, also the following linear combinations are valid eigenfunctions:

$$\Psi_{anti} = \Psi_a(1) \cdot \Psi_b(2) + \Psi_a(2) \cdot \Psi_b(1)$$

At the same time Pauli's principle has to be respected, that means the eigenfunction Ψ_{ant} contains additionally the anti-parallel spins (↑↓ + ↑↓) and the function Ψ_{sym} the parallel spins (↑↑- ↓↓). The electron distribution described by the linear combinations depends also on the distance dependent mutual electrostatic disturbance. As disturbance we have to consider the terms

$$\Delta U = -e^2 \cdot \left(\frac{1}{r_{b1}} + \frac{1}{r_{a2}} - \frac{1}{r_{ab}} \right)$$

which are the reason for the mutual interaction. To get the complete solution we have to add a „disturbance"-term to the undisturbed eigenfunctions Ψ_a and Ψ_s , as well as to the undisturbed energy. Then Schroedinger's equation will no more be homogeneous, but inhomogeneous because of the additional „disturbance" term. As solution we get:

$$E_{sym} = 2E_0 + e^2 \cdot C + e^2 \cdot A$$

$$E_{anti} = 2E_0 + e^2 \cdot C - e^2 \cdot A$$

We see, that a term with the constant C representing the Coulomb part and a term with the constant A representing the interaction are added to the undisturbed energy. The exchange energy is based on the fact, that electron 1 is localised near to nucleus A at a particular instant and near to nucleus B at another instant. The sign of A can be positive or negative. The energy difference between the two possible energies is just

$$\Delta E = E_{sym} - E_{anti} = 2 \cdot e^2 \cdot A$$

A detailed calculation results in the following relation for C:

$$C = \int \left(\frac{1}{r_{ab}} - \frac{1}{r_{a2}} - \frac{1}{r_{b1}} + \frac{1}{r_{12}} \right) \cdot \Psi_a^2(1) \cdot \Psi_b^2(2) d^3r$$

and for A:

$$A = \int \left(\frac{1}{r_{ab}} - \frac{1}{r_{a2}} - \frac{1}{r_{b1}} + \frac{1}{r_{12}} \right) \cdot \Psi_a(1) \Psi_b(2) \Psi_a(2) \Psi_b(1) \cdot d^3r$$

Under respect of the fact, that $\psi_a^2(1)$ and $\psi_b^2(2)$, integrated over the whole space, represents probability densities which, multiplied by the elementary charge e, provide the total charge density ρ of the electrons 1 or 2 near the nuclei A or B, the constant C can also be written as:

$$e^2 C = \frac{e^2}{r_{ab}} - \int \frac{e^2 \rho_1}{r_{b1}} d^3r_1 - \int \frac{e^2 \rho_2}{r_{b2}} d^3r_2$$

$$+ \iint \frac{e^2 \rho_1 \rho_2}{r_{12}} d^3r_1 d^3r_2$$

We see that C results out of the attracting or repulsing Coulomb forces. The exchange integral A looks very much like the Coulomb integral. But the electron densities $\psi^2_a(1)$ resp. ψ^2 (2) have been replaced by the mixed terms ψ_a(1) ψ_b (2) and ψ_a(2) ψ_b(1) which are the result of the electron exchange. Here we can summarize as follows: If atoms are mutually approached the states of the undisturbed energy levels split into energetically different states. The number of newly created energy states are corresponding to the number of exchangeable electrons. (Fig. 20).

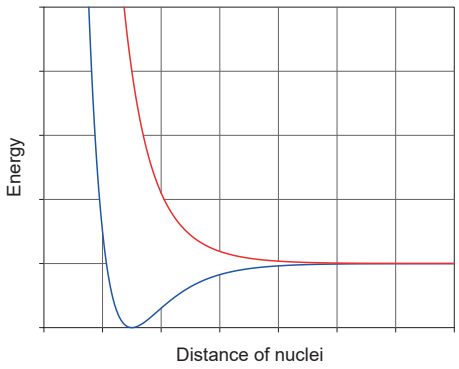

Fig. 2: Potential energy due to interaction of two hydrogen atoms

One of the curves shows a minimum for a particular distance of the atoms. Without being forced, the atoms will undoubtedly approach until they have acquired the minimum of potential energy. This is also why hydrogen always occurs as molecular hydrogen H2 under normal conditions. The second curve does not have such a distinct property. The curves distinguish the binding case in that the spins of the electrons are anti-parallel. For the non-binding case, they are parallel. It is easy to imagine that an increase in the number of atoms also increases the number of exchangeable electrons and, consequently, the number of newly generated energy levels. Finally, the energy levels are so high and so dense that we can speak about an energy band. Here, it is interesting to compare the electrons' action with the ambassadors' behavior.

The electrons in the outermost shell will learn first about the approach of an unknown atom. The eigenfunctions will overlap in a sense. One electron will leave the nucleus tentatively to enter an orbit of the approaching atom. It may execute a few rotations and then return to its original nucleus.

If everything is OK and the spins of the other electrons have adapted appropriate orientations, new visits are performed. Due to the visits of these "curious "electrons, the nuclei can continue their approach. This procedure goes on until the nuclei have reached their minimum acceptable distance. Meanwhile, it can no longer be distinguished which electron was part of which nucleus. If a significant number of nuclei have approached in this way, there will also be a significant number of electrons that are weakly bound to the nuclei. Still, there is one iron rule for the electrons: my energy level can only be shared by one electron with opposite spin (Pauli principle). Serious physicists may now warn to assume that there may eventually be male and female electrons. But who knows.....

Let's return to incorruptible physics.

Up to now we presumed that the atom only has one electron. With regard to the semiconductors to be discussed later this will not be the case. Discussing the properties of solid bodies it is sufficient to consider the valence electrons that means the most outside located electrons only as it has been done for separated atoms. The inner electrons bound closely to the nucleus participate with a rather small probability in the exchange processes. Analogously to the valence electrons of the atoms there is the valence band in solid bodies. Its population by electrons defines essentially the properties of the solid body. If the valence band is not completely occupied it will be responsible for the conductivity of elec-

trons. A valence band not completely occupied is called ***conduction band***.

If it is completely occupied the next not completely occupied band will be called conduction band.

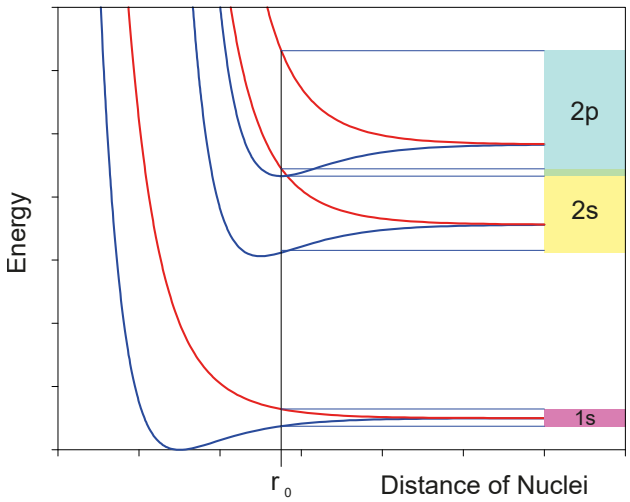

Fig. 3: Band formation by several electrons. The most outside electrons are responsible for the equilibrium distance r_0.

In the following section the question is to be answered how the density of states of a band of electrons looks like and on which quantities it depends. Before doing that and for reasons of completeness another attempt is made to determine the electron distribution within a solid body.

1.3.1 Periodic potentials

Although quantum mechanics is fairly powerful, up to now one has not succeeded to calculate the energy eigenvalues of complex atoms and molecules. One generally relies on skilful statements for the energy potentials to which the electrons are submitted. The statement of periodical potentials has been found to be especially powerful.

1.4 Fermi distribution

In Fig. 3 we have shown that the energy bands are the result of the mutual interaction of the atoms. Each band has a particular width ΔE, the magnitude of which is determined by the exchange energy and not by the number N of the interacting atoms. Furthermore we know that the number of energy levels within a band is determined by the number of interacting electrons. The Pauli principle states that such a level can only be occupied by two electrons. In this case the spins of the electrons are anti-parallel. Within a band the electrons are free to move and they have a kinetic energy of

$$E = \frac{1}{2} m v^2 \quad \text{or} \quad E = \frac{p^2}{2m}$$

The mass of the electron is m, v the velocity and p the impulse. The constant potential energy will not be taken into consideration. Furthermore we will set the energy of the lower band edge to zero. The maximum energy E_{max} of an electron within a band can not pass the value ΔE since otherwise the electron would leave the band and no longer be a part of it. Consequently we can write:

$$E_{max} = \Delta E = \frac{1}{2m} p_{max}^2$$

.

We still have to find out how many electrons of energy $E \leq E_{max}$ exist and within a second step we wish to know how many electrons exist in the energy interval dE. To reach this goal we will use a trick already applied in deriving the number of modes in a cavity resonator (see also LE-0100 Emission & Absorption). But here we will consider electrons instead of photons. The course of considerations will be the same since we can attribute to each electron a wave with wave vector k. For the impulse p we write:

$$\vec{p} = \hbar \cdot \vec{k}$$

Only such electron energies are permitted within a volume the wave functions of which are zero at the walls. To express it in a more simple way: an integer multiple of half the wavelength λ of the associated standing wave must fit, for instance, into the length L of a cube:

$$L_x = n_x \frac{\lambda}{2} \quad \text{and} \quad k_x = \frac{2\pi}{\lambda}$$

For the electron energy of the cube we get:

$$E = \frac{p^2}{2m} = \frac{\hbar^2}{2m} \vec{k} \cdot \vec{k} = \frac{\hbar^2}{2m} \left(k_x^2 + k_y^2 + k_z^2 \right)$$

$$E = \frac{2h^2}{m} \left(\frac{n_x^2}{L_x^2} + \frac{n_y^2}{L_y^2} + \frac{n_z^2}{L_z^2} \right) = \frac{2h^2}{mL^2} \left(n_x^2 + n_y^2 + n_z^2 \right)$$

Let's remember the equation of a sphere

$$R^2 = x^2 + y^2 + z^2$$

and compare it with the equation for E. We recognize an analogous equation of the following type:

$$E \frac{mL^2}{2h^2} = \left(n_x^2 + n_y^2 + n_z^2 \right)$$

or with :

$$E = \frac{\hbar^2 k^2}{2m}$$

$$L^2 \frac{k^2}{\pi^2} = n_x^2 + n_y^2 + n_z^2$$

The radius of this sphere is Lk/π and n_1, n_2, n_3 are the x y z coordinates. As n is an integer and positive they only generate one eighth of a complete sphere set up by a spatial lattice with lattice constant 1.

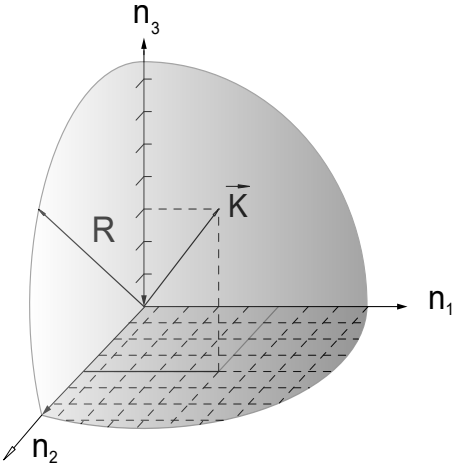

Fig. 4: Calculation of the electron density

Permissible are only such wave vectors , the components of which are coinciding with the n values or, to express it differently, each point of intersection of the lattice represents a valid solution for the wave vector k of a stationary wave. The answer to the initially raised question regarding the number of electrons for a particular length L of a potential box results now out of the counting of the number of points of intersection (Fig. 4).

This work can also be done analytically. If one uses the formula for the volume of a sphere $V_{sphere} = 4/3\ \pi\ R^3$ one gets for one eighth of a sphere with a radius for an upper limit of energy at E_{max}:

$$N(E_{max}) = \frac{1}{8}\cdot\frac{4}{3}\pi\cdot\left(L\frac{k}{\pi}\right)^3$$

with $E = \frac{\hbar^2 k^2}{2m}$ or $k^2 = \frac{4\pi^2}{h^2}2mE$ one gets:

$$N(E) = \frac{8}{3}\frac{\pi}{h^3}V\cdot(2mE)^{3/2}$$

Here V is the volume of the box. An additional factor of 2 accounts for the fact that two electrons are admitted in each state if their spins are anti-parallel. Let's divide *N(E)* by the volume V to get the electron density

$$n(E) = \frac{8}{3}\frac{\pi}{h^3}\cdot(2mE)^{3/2}$$

The electron density per unit energy dn(E)/dE is found by differentiation:

$$dn(E) = \frac{4\pi}{h^3}(2m)^{3/2}\sqrt{E}\cdot dE$$

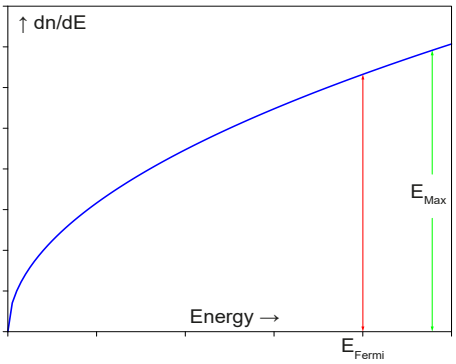

Fig. 5: Number of electrons per unit volume V and energy interval dE as a function of the energy E.

The situation in Fig. 5 shows that the band has not been completely filled up since the Fermi energy is smaller than the maximal possible energy. This means that this band is a conduction band. If the Fermi energy would be equal to the maximal energy we would have a valence band. A transfer of this knowledge to the energy level scheme of Fig. 3 and a selection of the 2s band would provide the picture of Fig. 6. Up to this point we anticipated that the temperature of the solid body would be 0 K. For temperatures deviating from this temperature we still have to respect thermodynamic aspects namely additional energy because of heat introduced from outside. Fermi and Dirac described this situation using statistical methods. The electrons were treated as particles of a gas: equal and indistinguishable. Furthermore it was presumed that the particles obey the exclusiveness principle which means that any two particles can not be in the same dynamic state and that the wave function of the whole system is anti-symmetrical.

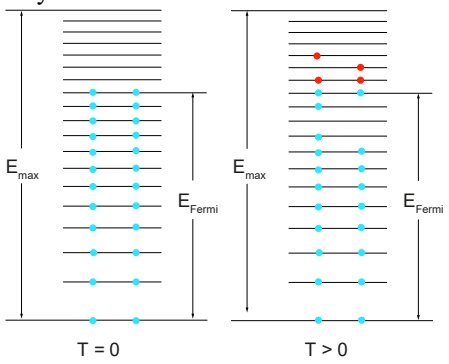

Fig. 6: Fig. 6: Distribution of free electrons over the energy states within a conduction band

Particles which satisfy these requirements are also called Fermions. Correspondingly all particles which have a spin of 1/2 are Fermions and obey the Fermi Dirac statistics. Electrons are such particles. Under respect of these assumptions both physicists got the following equation for the particle density of the electrons within an energy interval dE:

$$\frac{dn(E)}{dE} = \frac{4\pi}{h^3}(2m)^{3/2}\cdot\frac{\sqrt{E}}{e^{\frac{E-E_{Fermi}}{kT}}+1}\cdot dE$$

The above equation is illustrated by Fig. 7. As shown in Fig. 6 by introduction of thermal energy the „highest" electrons can populate the states which are above them. Based on these facts we are well equipped to understand the behavior of solid bodies. We are going to concentrate now our special interest on the semiconductors which will be presented in the next chapter with the help of the previously performed considerations.

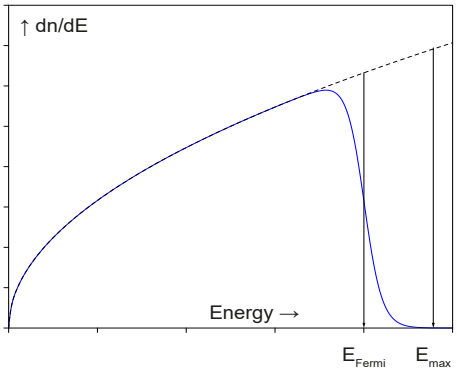

Fig. 7: Number of electrons per unit volume and energy interval dE as a function of the energy E, but for a temperature T > 0.

1.5 Semiconductors

Before starting the description of the semiconductor with regard to its behavior as „lasing" medium we still have to study the „holes". States of a band which are not occupied by electrons are called „holes". Whenever an electron leaves its state it creates a hole. The electron destroys a hole whenever it occupies a new state. The whole process can be interpreted in that way that the hole and the electron exchange their position (Fig. 7). Also the holes have their own dynamic behavior and can be considered as particles like the electrons. It is interesting to note that the holes do have the exact opposite

properties of the electrons. Since the temporary course of the holes' migration is the same as for the electron they have also the same mass except that the mass of the hole has the opposite sign. Furthermore its charge is positive.

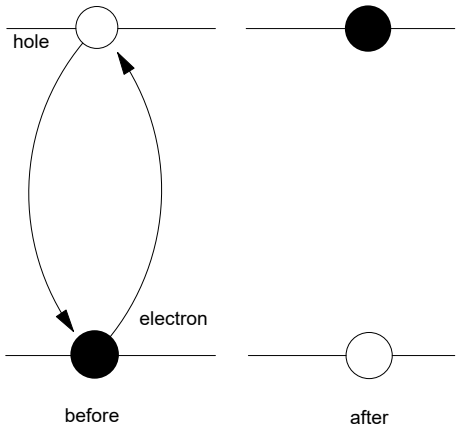

Fig. 8: Electron and hole transition

Once the existence of the holes has been accepted they also have to have a population density. It will be introduced in the following. For this reason we complete Fig. 6 as shown in Fig. 9.

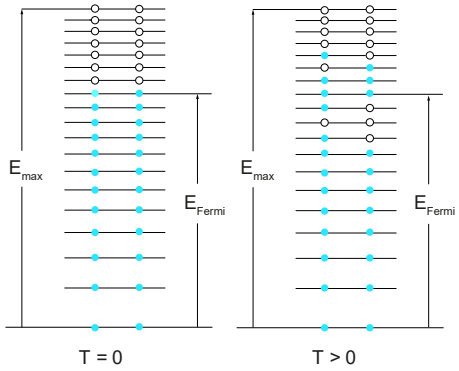

Fig. 9: Distribution of the holes and the electrons within an energy band

It is easy to understand that on one side the holes are preferably at the upper band edge and on the other side their population density results out of the difference of the population density minus the population density of the electrons. Fig. 10 shows the population density of the electrons. Fig. 11 shows the difference and in so far the population density of the holes. Attention has to be paid to the fact that the abscissa represents the energy scale of the band and not the energy of the holes.

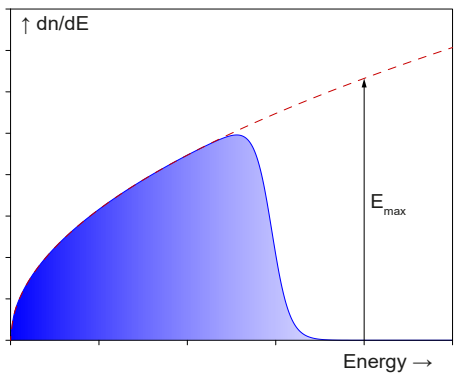

Fig. 10: Population density of the electrons

To prepare the discussion of optical transitions in semiconductors it gives a sense to modify the diagrams. Until now the abscissa was used as energy scale for the diagrams of the state and population densities. For the presentation of optical transitions it is more practical to use the ordinate as energy scale. To get use to it Fig. 10 has been represented in the modified way in Fig. 12. The shown population density refers to an energy scale for which the lower edge of the valence band has been set arbitrarily to zero. The represented situation refers to a semiconductor where the distance between conduction and valence band is in the order of magnitude of thermal energy *(kT)*. Here the Fermi energy lies in the forbidden zone.

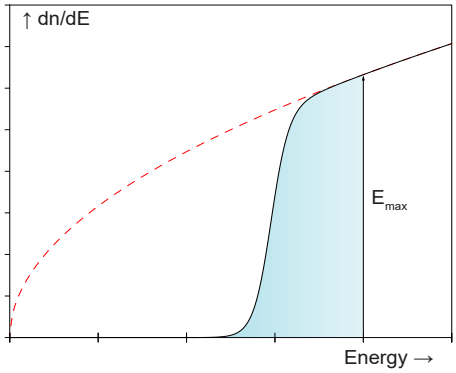

Fig. 11: Population density of the holes

Because of the thermal energy some electrons have left the valence band and created holes. For the following considerations it is sufficient to learn something about the population densities of the electrons in the conduction band as well as about the holes in the valence band. As will be shown later there are optical transitions from the conduction band to the valence band provided they are allowed. Near the lower band edge of the conduction band the state densities are admitted to be parabolic. The same is true for the holes at the upper edge of the valence band (Fig. 13). The densities of states inform about the number of states which are disposed for population and the spectral distribution reflects how the electrons and holes are distributing over these states. Next to the band edges the spectral distribution fits to a Boltzmann distribution.

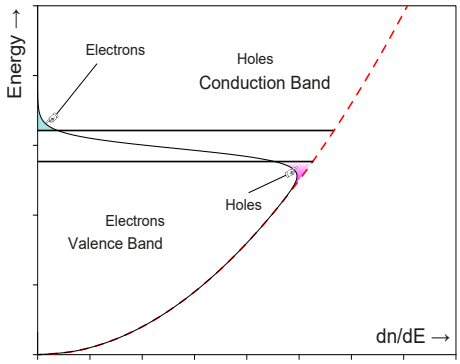

Fig. 12: Population density on the energy scale

If we succeed to populate the conduction band with electrons and to have a valence band which is not completely occupied by electrons (Fig. 13) electrons may pass from the conduction band to the valence band. That way a photon is generated. By absorption of a photon the inverse process is also possible.

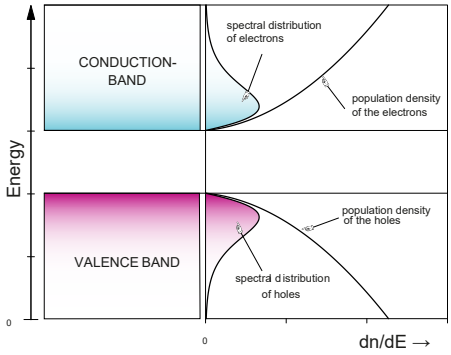

Fig. 13: Densities of states and spectral distributions

The following illustration Fig. 14 shows the situation of a population inversion in a semiconductor. Attention must be drawn to the fact that, until now, we only discussed a semiconductor consisting of one type of atoms. Consequently the situation shown in Fig. 14 is, at least for this type of direct semiconductor, only fictitious. It can only be created for very short intervals of time and can therefore not be taken into consideration for the realization of a semiconductor laser. By doping the basic semiconductor material we can create band structures with different properties. A very simple example may be the semiconductor diode where the basic material, germanium or silicon, is converted into p or n conducting material using suitable donators and acceptors. By the connection of the doted materials a barrier (also called active zone) is formed. It will be responsible for the properties of the element. Silicon is mainly used for highly integrated electronic circuits while ZnS is chosen as fluorescent semiconductor for TV screens. As light emitting diodes and laser diodes so called mixed semiconductors like AlGaAs are in use. Mixed semiconductors can be obtained whenever within the semiconductors of valence three or five individual atoms are replaced by others of the same group of the periodical system. The most important mixed semiconductor is aluminum gallium arsenide (AlGaAs), where a portion of the gallium atoms has been replaced by aluminum atoms. This type of semiconductor can only be produced by a fall out as thin crystal layer, the so called epitaxy layer, on host crystals. To perform this stressfree it is important that the lattice structure of the host crystal (lattice matching) coincides fairly well with the lattices structure of AlGaAs. This is the case for GaAs substrate crystals of any concentration regarding the Al and Ga atoms within the epitaxy layer. In that way the combination of AlGaAs epitaxy layers and GaAs substrates offers an ideal possibility to influence the position of the band edges and the properties of the transitions by variation of the portions of Ga or Al.

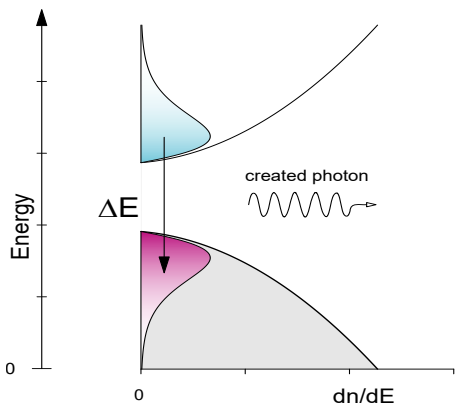

Fig. 14: Population inversion in a semiconductor for T > 0

1.1 *Semiconductor laser*

As simple as it may seem, it took about 20 years until people had acquired the necessary technology of coating under extremely pure conditions. It all began in 1962 with the first laser diode, just two years after Maiman had demonstrated the first functional ruby laser. In the course of 1962 three different groups reported more or less simultaneously the realisation of GaAs diode lasers.

1.	R. N. Hall	General Electric
2.	M. I. Nathan	IBM
3.	T. M. Quist	MIT

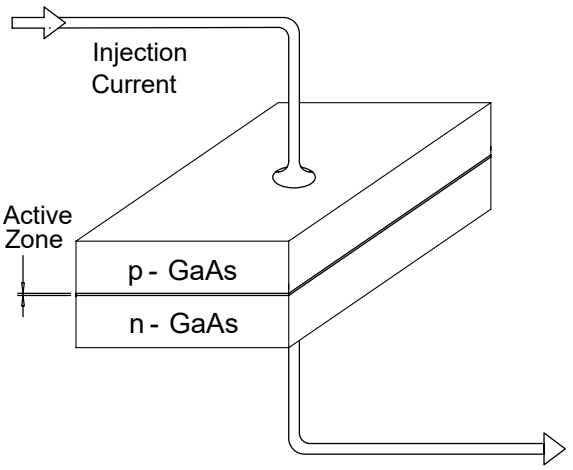

Fig. 15: Simple laser diode around 1962, working at 70 K and with 100 kA/cm2 in the pulse mode.

The first laser was basically made of highly doted GaAs (Fig. 15). A threshold current of 100 kA/cm^2 was needed since the GaAs material of those days was not by far as good as it is today regarding the losses within the crystal. Because of thermal conditions the laser could only work at 70 ^{0}K and in the pulsed mode. In the course of the following years the threshold could be lowered to 60 kA/cm^2 by improving the crystals but only the use of a hetero-transition (Bell Labs. and RCA-Labs.) brought the „break-through“ in 1968. The threshold could be lowered to 8 kA/cm^2 and working in the pulse mode at room temperature was possible (Fig. 16).

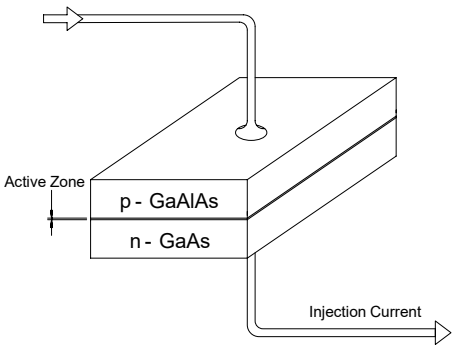

Fig. 16: Simple hetero-structured laser around 1968, working at 8 kA/cm2 in pulse mode at room temperature.

In this concept a layer of p conducting GaAlAs is brought on the p layer of the pn transition of GaAs. The slightly higher band gap of GaAlAs compared to GaAs ensures that a potential barrier is created between both materials in a way that charge carriers accumulate here and the formation of inversion is increased respectively the laser threshold is remarkably lowered to 8 kA/cm^2 .

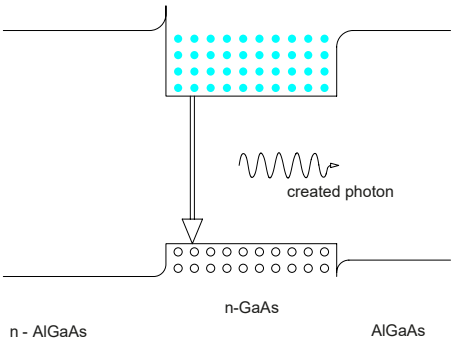

Fig. 17: Energy band diagram of a N n P - double hetero structure.

The next step in development was the attachment of a similar layer on the n-side of the crystal. That way the threshold could be lowered once again in 1970. Now it amounted to about 1 kA/cm^2. Until today nearly all commercially sold laser diodes are built up on the double hetero structure principle (Fig.18 and Fig. 19).

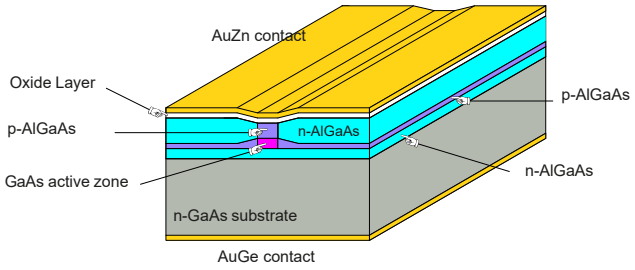

Fig. 18: „Buried“ hetero structure. The active zone has been buried between some layers which ensure an optimal beam guidance in the zone.

1.2 *Resonator and beam guidance*

As already mentioned at the beginning the diode laser differs from the „classical“ lasers in the dimensions of the resonator and in the propagation of the beam. For the diode lasers the active material represents the resonator at the same time. Furthermore the ratio of the resonator length (300 µm) to the wavelength (820 nm) is:

$$L / \lambda = 366 ,$$

For a HeNe-Laser (λ = 632 nm) with a typical resonator length of 20 cm this ratio is 3 $10^{8.}$ Considering additionally the lateral dimensions of the resonator we get a ratio of 12.5 for the diode lasers with a typical width of 10 µm for the active zone. With capillary diameters of the He-Ne tubes of about 1 mm one gets a value of 1582. This already indicates that the beam characteristics of the laser diode will distinguish significantly from „classical“ lasers.

1.3 *Divergence and intensity distribution*

Not only the beam guidance but also the size of the laser mirrors influences the beam geometry. Generally for conventional lasers the mirrors are very large compared with the beam diameter. The laser mirror (crystal gap area of the active zone) of the laser diodes has a size of about 10 µm x 2 µm, through which the laser beam has „to squeeze“ itself. Diffraction effects will be the consequence and lead to elliptical beam profiles (Fig. 19).

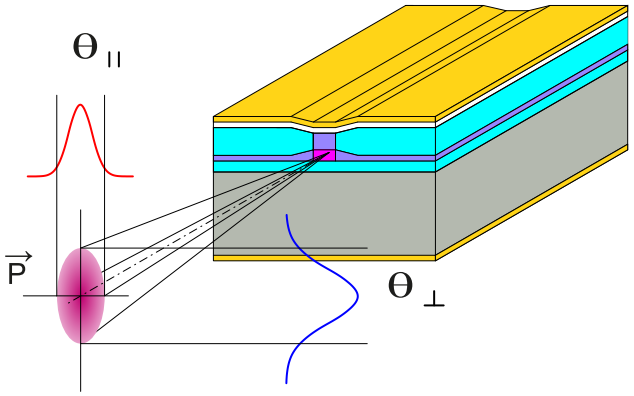

Fig. 19: Elliptical beam profile of a diffraction limited laser diode in the far field (some meters).

The polarization is parallel to the “junction plane”, that is the plane which is passed by the injection current perpendicularly. The divergence angles $\theta_\perp$ and $\theta_\parallel$ differ by about 10-30° depending on the type of laser diode.

If the beams are extended geometrically into the active medium the horizontal beams will have another apparent point of origin as the vertical beams. The difference between the points of origin is called astigmatic difference (Fig. 20). It amounts to about 10 µm for the so called index guided diodes. For the so called gain guided diodes these values are appreciably higher.

Modern diodes are mostly index guided diodes. This means that the laser beam is forced not to leave the resonator laterally by attaching lateral layers of higher refractive index to the active zone. At the gain guided diodes the current is forced to pass along a small path (about 2-3 µm width).

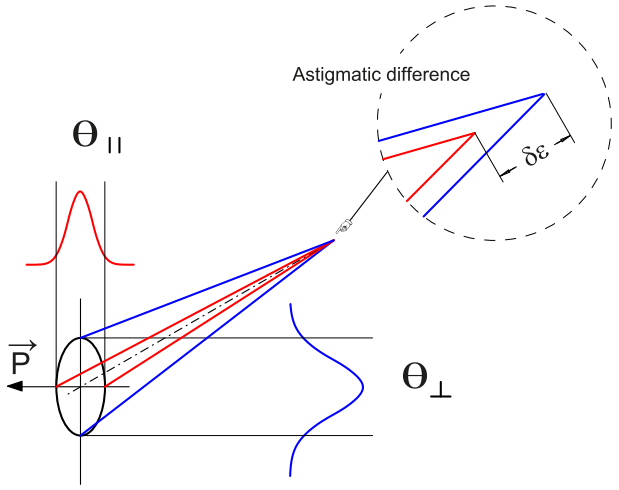

Fig. 20: Astigmatic difference $\delta\varepsilon$

In this way the direction of the amplification (which is proportional to the current flux) and the laser radiation are determined.

At the gain guided diodes the formation of curved wave fronts within the resonator is disadvantageous since they simulate spherical mirrors. In this case higher injection currents provoke transversal modes which will not appear in index guided diodes because of the plane wave fronts. Laser diodes with intensity profiles following a Gauss curve and a beam profile which is only limited by diffraction are called ***Diffraction Limited Lasers*** (DFL).

They represent the most „civilized“ diode lasers. For the time being they are only available for powers up to 200 mW. High power diode lasers as used, for example, to pump Nd YAG lasers partially have very fissured nearly rectangular intensity profiles.

1.6 Polarisation

It is understandable that the laser radiation of the diodes has a distinct direction of polarization, since the height of the exit window is 4 times and the width 12.5 times larger than the wavelength.
Because of the fraction of spontaneous emission the light of the laser diode also contains components oscillating in the vertical direction
The ratio of polarization, $P_{\perp}$ to $P_{\parallel}$, depends on the output power since for higher laser power the ratio of spontaneous to stimulated emission is changing (Fig. 22).

1.7 Light Emitting Diodes (LED)

An LED (light-emitting diode) is built around a PN junction, two semiconductor regions joined together. The P-type side is rich in “holes” (positive charge carriers), while the N-type side has excess electrons (negative carriers). When you apply a forward voltage, electrons from the N-side and holes from the P-side are pushed toward the junction. As these carriers meet at the junction, electrons drop into holes, filling them and releasing energy. In an LED, that energy is emitted as photons rather than as heat as in an ordinary diode.
The color of the emitted light depends on the semiconductor’s band gap, the energy difference between its conduction and valence bands. A larger band gap means higher-energy (shorter-wavelength) photons, blue or ultraviolet light, while a smaller gap yields red or infrared light.
Common materials include gallium arsenide (GaAs) for infrared LEDs, gallium phosphide (GaP) for red and green, and gallium nitride (GaN) for blue. By precisely controlling the chemical composition and crystal structure, manufacturers fine-tune the band gap and therefore the LED’s color.

2 Experimental Setup and Components

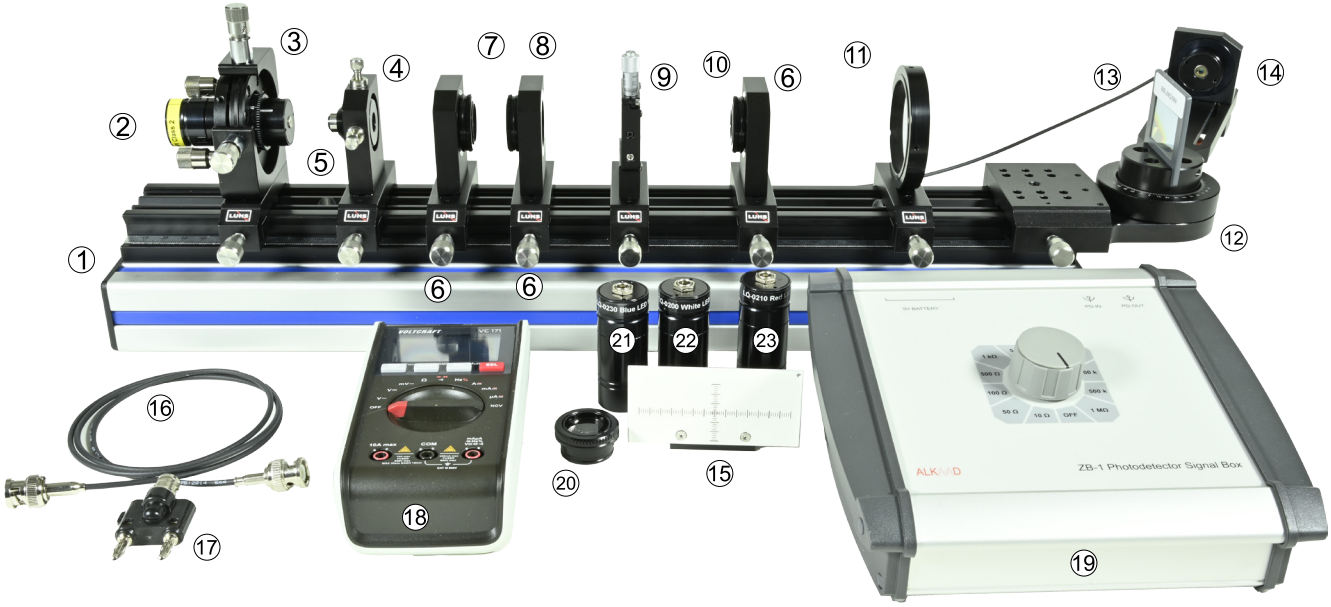

Fig. 21: Description of the components

1	MP-0150 Optical Bench MG-65, 500 mm	13	OC-0460 Transmission grating 600 l/mm
2	LQ-0060 Red (635 nm) diode laser in ø 25 housing	14	DC-0120 Si-PIN Photodetector, BPX61
3	MM-0216 4-axes adjustment holder on MG20	15	MP-0220 White screen with XY scale on block
4	MM-0090 XY adjuster on MG20	16	CA-0450 BNC connection cable 1 m (2x)
5	OC-0190 Collimator VIS in Collimator mount	17	CA-0410 BNC - banana adapter 19 mm
6	MM-0020 Mounting plate C25 on carrier MG20	18	CA-0220 Multimeter 3 1/2 digits
7	OC-0220 Cylindrical lens f = -15 mm in C25 mount	19	DC-0380 Photodetector Junction Box ZB1
8	OC-0280 Cylindrical lens f=45 mm in C25 mount	20	OC-0040 Plano-convex lens f=40 mm in C25 mount
9	MM-0240 Adjustable slit on carrier 20 mm	21	LQ-0230 Blue LED in ø 25 housing
10	OC-0040 Plano-convex lens f=40 mm in C25 mount	22	LQ-0200 White LED in ø 25 Housing
11	MM-0110 Translucent screen on carrier MG20	23	LQ-0210 Red LED in ø 25 housing
12	MM-0300 Carrier with 360° rotary arm		

2.1 The rail and carrier system (1)

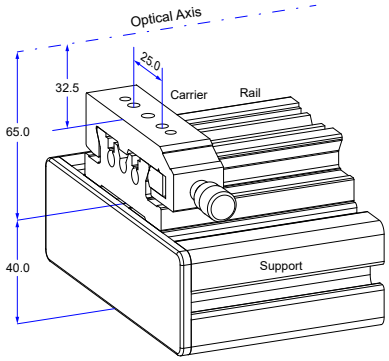

The rail and carrier system provides a high degree of integral structural stiffness and accuracy. Due to this structure, it is a further development optimized for daily laboratory use. The optical height of the optical axis is chosen to be 65/105 mm above the table surface. The optical height of 32.5 mm above the carrier surface is compatible with all other systems like from MEOS, LUHS, MICOS, OWIS and LD Didactic. Consequently, a high degree of system compatibility is achieved. The attached support elevates the working height above the table and significantly improves the handling of the components.

2.2 LQ-0060 Red (635 nm) diode laser (2), MM-0216 4-axes adjustment holder(4)

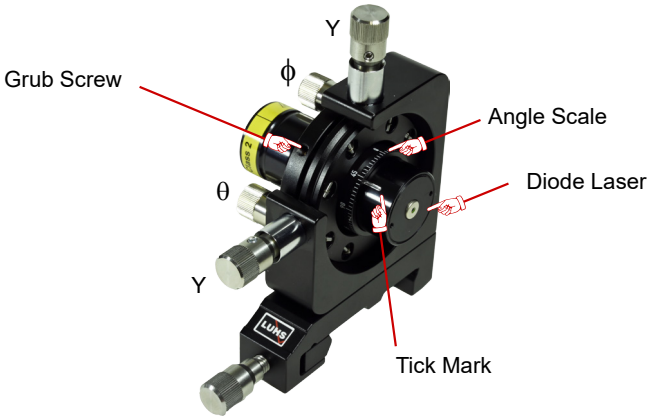

This adjustment holder provides a free opening of 25 mm in diameter. All components like the optics holder and laser (2) as well as LED (3) light sources can be placed into it. A spring loaded ball keeps the component in position. By means of high precision fine pitch screws the inserted component can be tilted azimuthal and elevational (C and D) and shifted horizontally (B) and vertically (A). With the attached carrier this unit can be placed onto the provided rails.

If needed, the light source can be locked withe the nylon tipped grub screw.

2.3 MM-0090 XY adjuster (4) and OC-0190 Collimator VIS in Collimator mount (5)

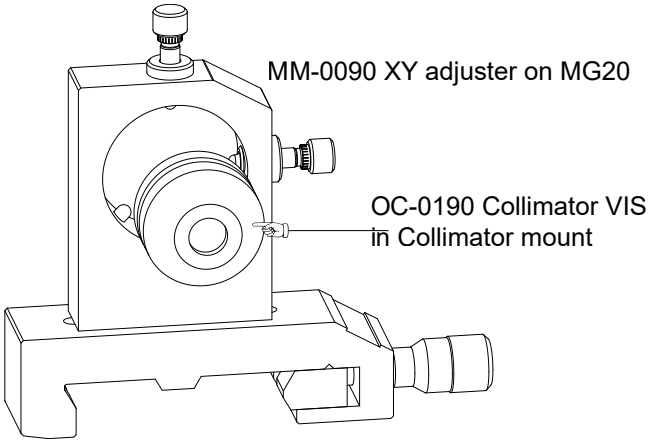

A high precision aspheric glass lens is mounted into a collimator mount which is inserted into the XY adjuster. With the fine pitch screws the collimator (OC-0190) can be adjusted accordingly. The glass lens has a focal length of 9.6 mm, the numerical aperture is 0.53 and the clear opening is 4,9 mm. In addition, the lens has an anti-reflex coating in a spectral range of 350 - 700 nm with a residual reflection of < 0.5 %.

2.4 MM-0020 Mounting plate C25 on carrier MG20 (6)

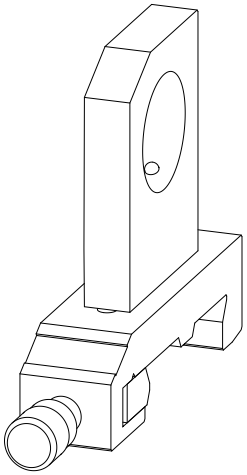

This frequently used component is ideal to accommodate parts with a diameter of 25 mm where it is kept in position by three spring loaded steel balls. Especially C25 mounts having a click groove are firmly pulled into the mounting plate due to the smart chosen geometry. The mounting plate is mounted onto a 20 mm wide carrier.

2.5 OC-0220 Cylindrical lens f = -15 mm (7) and OC-0280 Cylindrical lens f=45 mm (8)

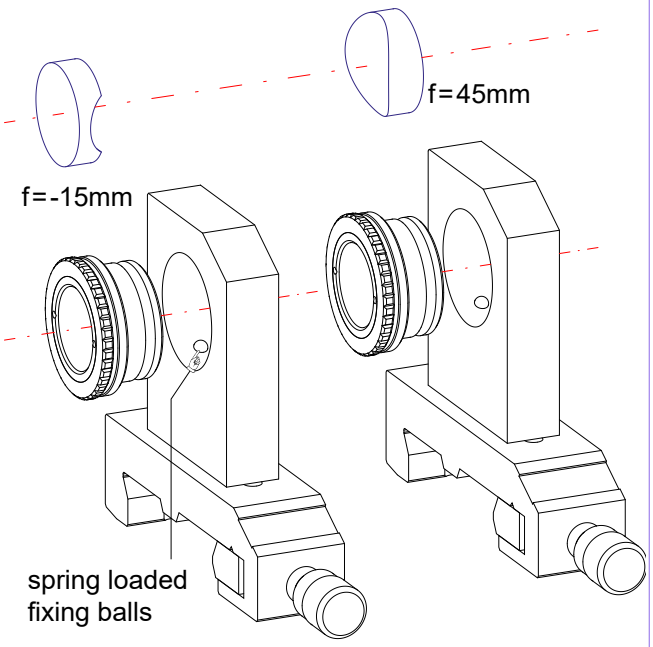

Optics for beam shaping consisting of a cylindrical lens with f=-15 mm and f=45 mm mounted in a click mount and a mounting plate on carrier.

2.6 MM-0240 Adjustable slit on carrier 20 mm (9)

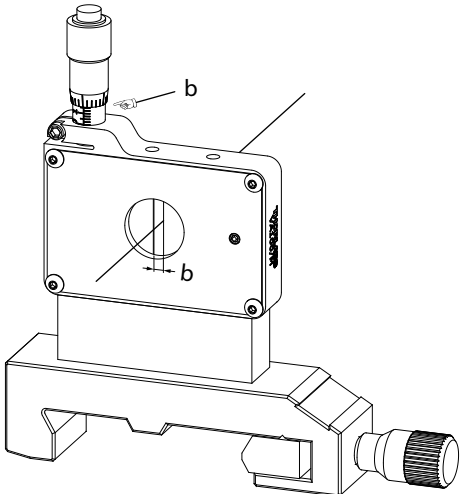

The mechanical slit provides precise adjustment of two blades centered equally about an through hole. Each blade is black to reduce unwanted reflections. The unique design provides a 1-to-1 correlation between the adjustment of the precision micrometer drive and the subsequent change in slit width to within 20 µm. The actual slit width (b) ranges from fully closed to 6 mm wide with 0.5 mm of adjustment per revolution.

2.7 OC-0040 Plano-convex lens f=40 mm in C25 mount (10 and 20)

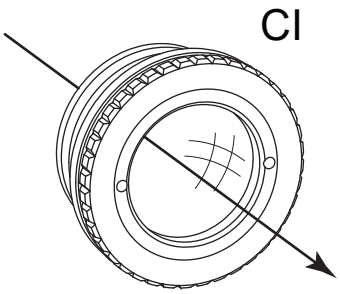

The mounted lens has a focal length of 40 mm and is mounted into a 25 mm click mount (CI) which can be inserted in any 25 mm mounting plate (6). It is used to image the diffraction pattern.

2.8 MM-0110 Translucent screen on carrier MG20 (11)

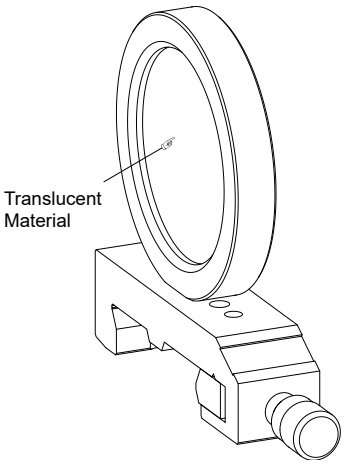

In a round holder a sheet of translucent paper is fixed with a retaining ring. This component is useful to image and visualize optical rays. Furthermore, the translucence allows the convenient photographic recording from the opposite side with digital cameras for a quick picture for the students measurement report.

2.9 MM-0300 Carrier with 360° rotary arm (12)

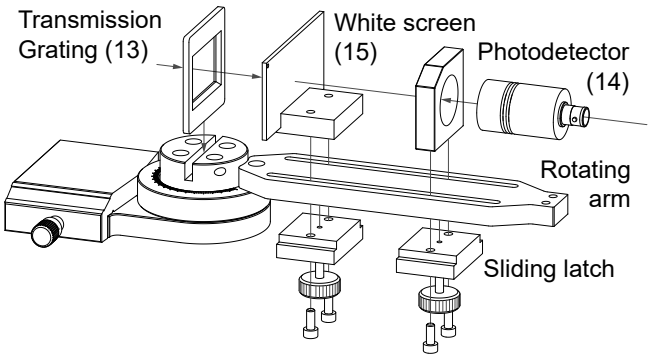

The goniometer consists of the fixed part which is attached at the end of the optical rail with a carrier. On top of the carrier a grating holder is mounted. A rotating arm is fixed to the goniometer and carries a movable mounting plate to accommodate the photodetector. The mounting plate can be moved along the arm when loosening the lock screw and locked in the desired position. In addition a white screen is placed and fixed in the same way as the photodetector.

2.10 DC-0120 Si-PIN Photodetector (14)

A Si PIN photodiode is integrated into a 25 mm housing with two click grooves (PD). A BNC cable and connector is attached to connect the module to the photodetector signal box ZB1. The photodetector module is placed into the mounting plate (MP) where it is kept in position by three spring loaded steel balls.

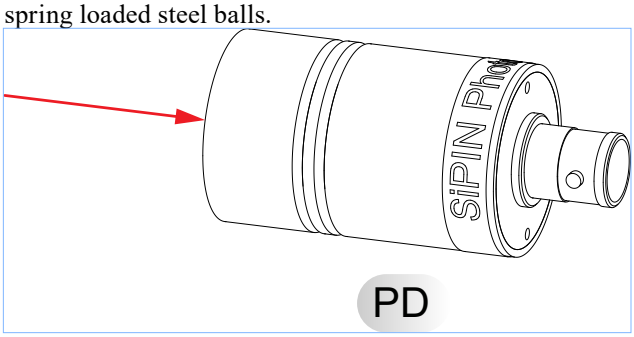

Fig. 22: Photodetector module

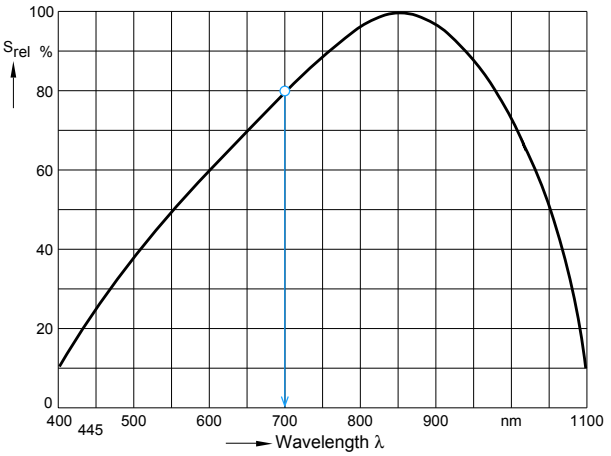

Fig. 23: Sensitivity curve of the BPX61 photodiode

Parameter	symbol	value
Rise and fall time of the photo current at: R_L=50 Ω, V_R=5V, λ=850 nm and Ip=800 µA	t_r, t_f	20 ns
Forward voltage I_F = 100 mA, E = 0	V_F	1.3 V
Capacitance at V_R = 0, f = 1 MHz	C_0	72 pF
Wavelength of max. sensitivity	λ_{Smax}	850 nm
Spectral sensitivity S~10% of S_{max}	λ	1100
Dimensions of radiant sensitive area	L x W	7 mm²
Dark current, V_R = 10 V	I_R	≤30 nA
Spectral sensitivity, λ = 850nm	$S(\lambda)$	0.62 A/W

Table 1: Basic parameters of Si PIN photodiode BPX61

2.11 DC-0380 Photodetector Junction Box ZB1 (19)

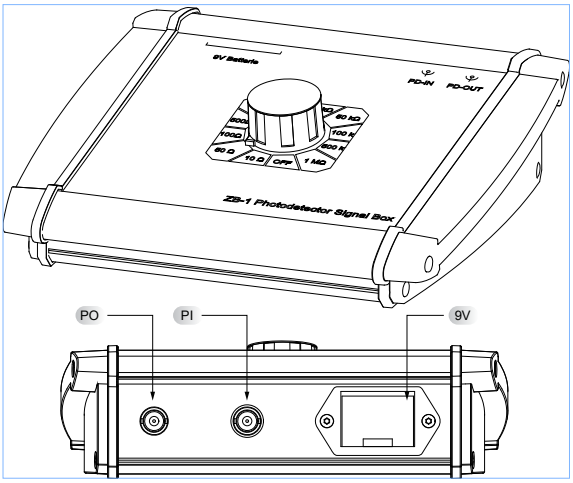

Fig. 24: Photodetector Signal Box ZB1

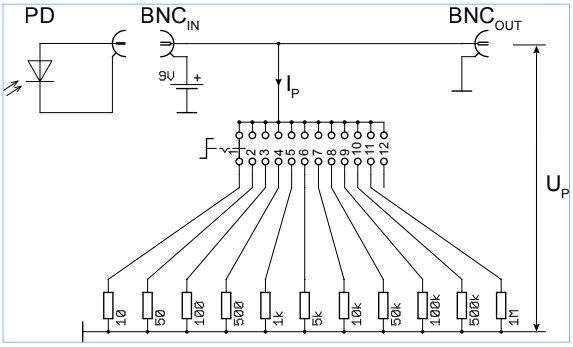

Fig. 25: Signal box schematic

The signal box contains a resistor network and a replaceable 9V battery and is prepared to accept all kinds of photodiodes provided they are connected to the BNC input (PD_{IN}) as shown in the schematic of Fig. 25. At the output PD_{OUT} of the signal box a signal is present which is given by the following equation:

$$Ip = \frac{Um}{R_L}$$

I_P is the photocurrent created by illuminating the photodiode with light.
U_m is the voltage drop across the selected load resistor R_L.
To convert the measured voltage into a respective optical power we have to make use of the spectral sensitivity S(λ) [A/W] which depends on the wavelength of the incident light according to Fig. 23. The detected optical power P_{opt} in W can be given as:

$$P_{opt} = \frac{I_p}{S(\lambda)}$$

Assuming a wavelength of 700 nm we take the value of S_{rel} from Fig. 23 as 0.8 and subsequently the value of $S(\lambda=700nm)$ is 0.62 x 0.8 = 0.496
If we are measuring a voltage U_m of 1V with a selected resistor R_L of 1K the optical power will be

$$P_{opt} = \frac{I_p}{S(\lambda)} = \frac{U_m}{R_L \cdot S(\lambda)} = \frac{5}{1000 \cdot 0.496} = 10\,mW$$

It must be noted that the measured power is correct only if the entire light beam hits the detector.

2.12 LQ-0230 Blue LED in ø 25 housing

An LED is installed in a 25mm-diameter housing. The housing features two grooves that engage with the spring-loaded balls of the mounting plate, providing a secure hold. The LEDs operate with a constant current of 500 mA. The integrated electronics are supplied with 12 volts of direct current via the built-in socket. The panel mounting socket has an outer diameter of 5.5 mm and an inner pin diameter of 2.5 mm. This experiment uses a blue (21), white (22), and red LED (23), as well as a red laser diode (2). The respective emission spectra are shown in the Fig. 26.

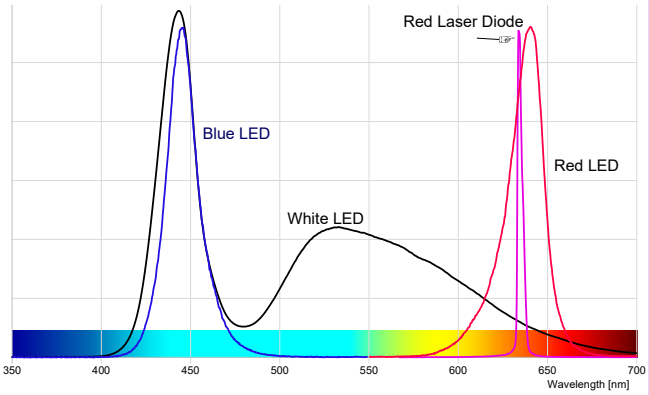

Fig. 26: Emission spectra of the used LED and Laser diode

3 Setup and Measurements

3.1 Spatial Intensity Distribution of the LED and Laser diode

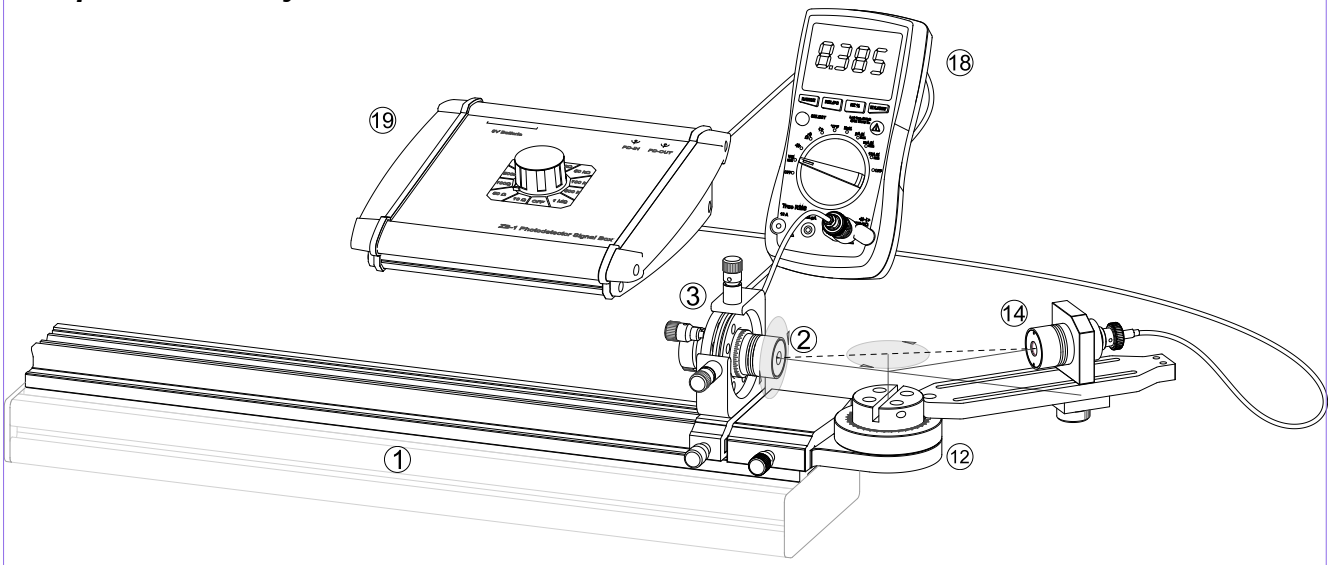

In this experiment, we measure the spatial intensity distribution of the laser diode or LED. The beam characteristic of the laser diode is elliptical while that of the LED is circular. The LED or laser diode (2) is inserted into the holder (4) and secured with the grub screw. The housing of the laser diode has a line mark to indicate the direction of rotation. The photodetector (14) is inserted into the mounting plate on the rotating arm, where it is held in place by the three spring-loaded balls on the mounting plate. The photodetector is connected to the photodiode connection box (19) using the BNC cable. The shunt resistor is selected so that a sufficiently high signal voltage is available and the photodiode is not saturated. The photovoltage is measured with the digital voltmeter (18), which is connected to the output of the photodiode connection box with a BNC cable.
The rotating arm is adjusted in 5° steps and the respective intensity is measured and noted until no measurable photovoltage is recognizable. Then rotate the laser diode by 90° and repeat the measurements.

3.2 Collimation of the Laser diode

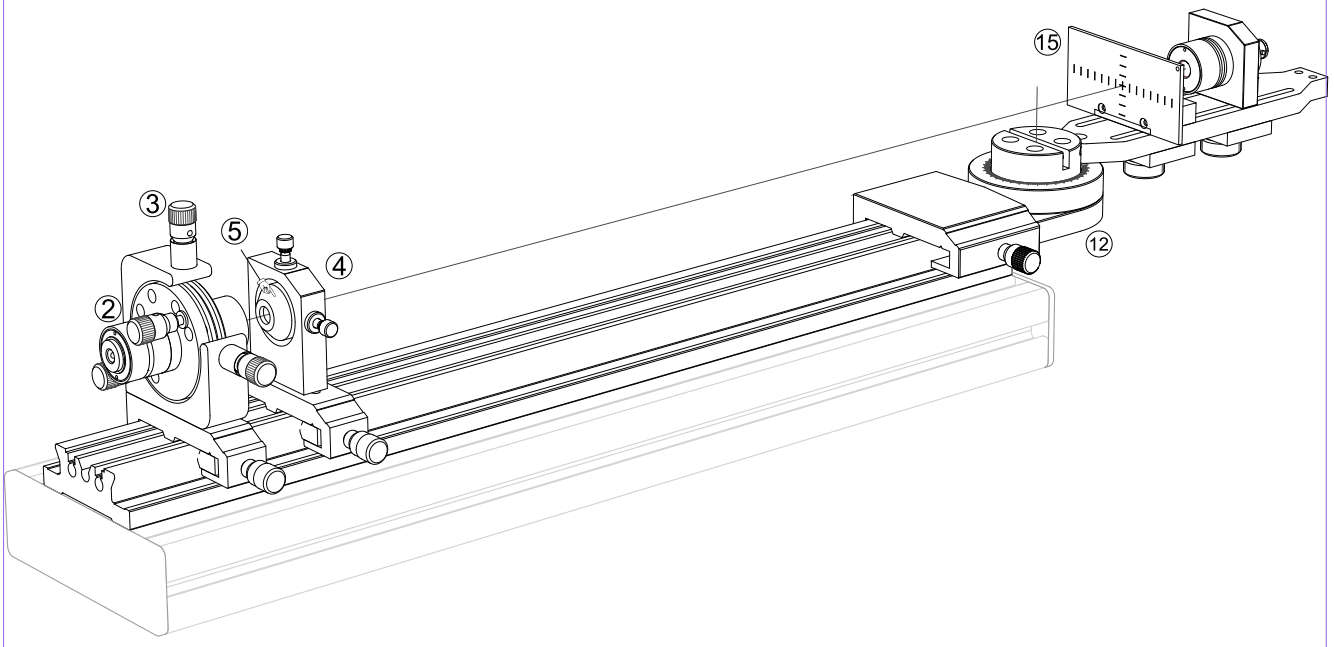

From the previous measurement we observed the strong divergence of the laser diode. The aim of this experiment is to collimate the emission of the laser diode. For this we use the collimator (5) with a focal length of 9.5 mm. The aim of this experiment is to generate a beam that is as parallel as possible. Using the adjustment screws of (3) and (4), the direction can be set so that the beam hits the center of the target. You can check the parallelism along the optical axis of the beam with a piece of paper.

Although the laser beam has become almost parallel, it still has an elliptical shape. In the following experiment we will try to shape the elliptical into a round beam profile.

3.3 Beam shaping of the Laser diode

3.3.1 Convert the Laser Dot into a Laser Line

For some applications, it is desirable for the laser to form a line instead of a dot. This is achieved by sending the round laser beam through a cylindrical lens. This is done in the following experiment. In the previous experiment we collimated the laser beam of the laser diode. Now we place a cylindrical lens (f=45mm) behind the collimator and image the beam on the imaging screen.

3.3.2 Convert the elliptical to a circular beam shape

From the previous measurements we have seen that despite good collimation the laser beam has an elliptical beam profile. For a variety of applications such as material processing or optical pumping, it is desirable to have a round beam profile. The aim of the next experiment is beam shaping with cylindrical lenses. For this we will build a cylindrical lens telescope with an expansion ratio of 1:3

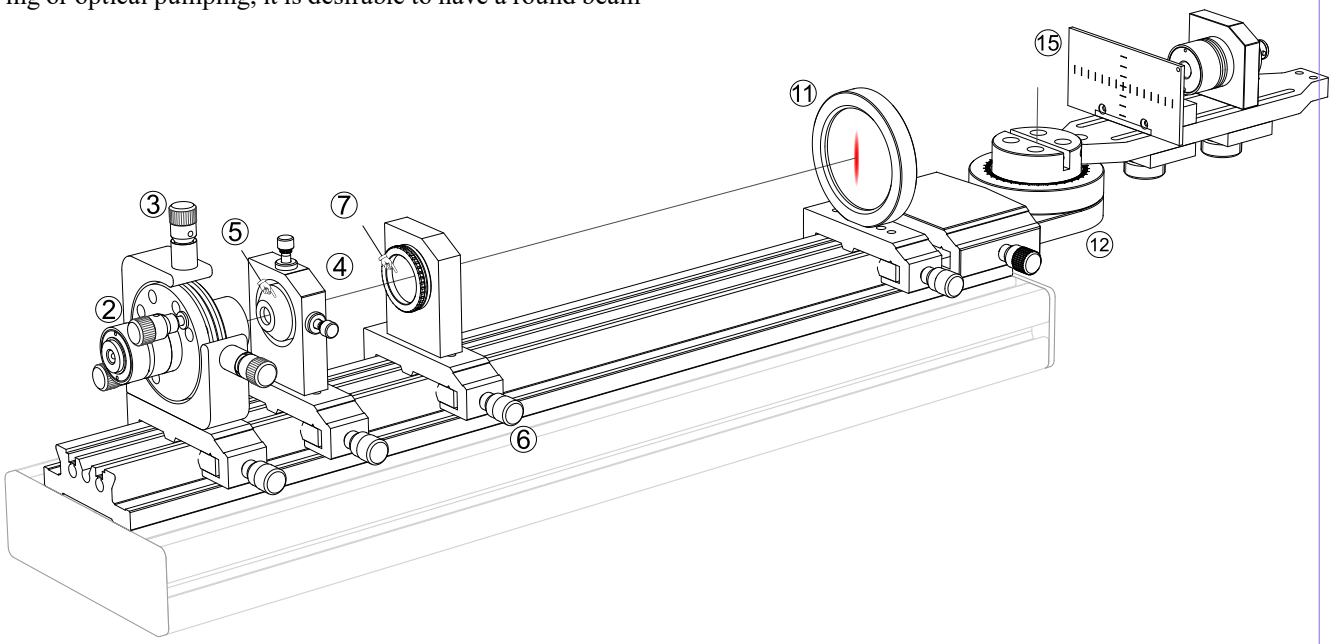

We place a plano-concave cylindrical lens (8) with a focal length of -15 mm in the setup with collimated laser beam. This produces a vertical line on the observation screen (11). If this is not the case, first check how the laser diode is oriented. To do this, look at the beam profile without the cylindrical lens on the observation screen and, if necessary, rotate the laser diode to obtain a vertical alignment. The laser diode is then fixed back into the holder with the grub screw. You can also rotate the cylindrical lens in the holder until a nice vertical profile is visible on the screen.

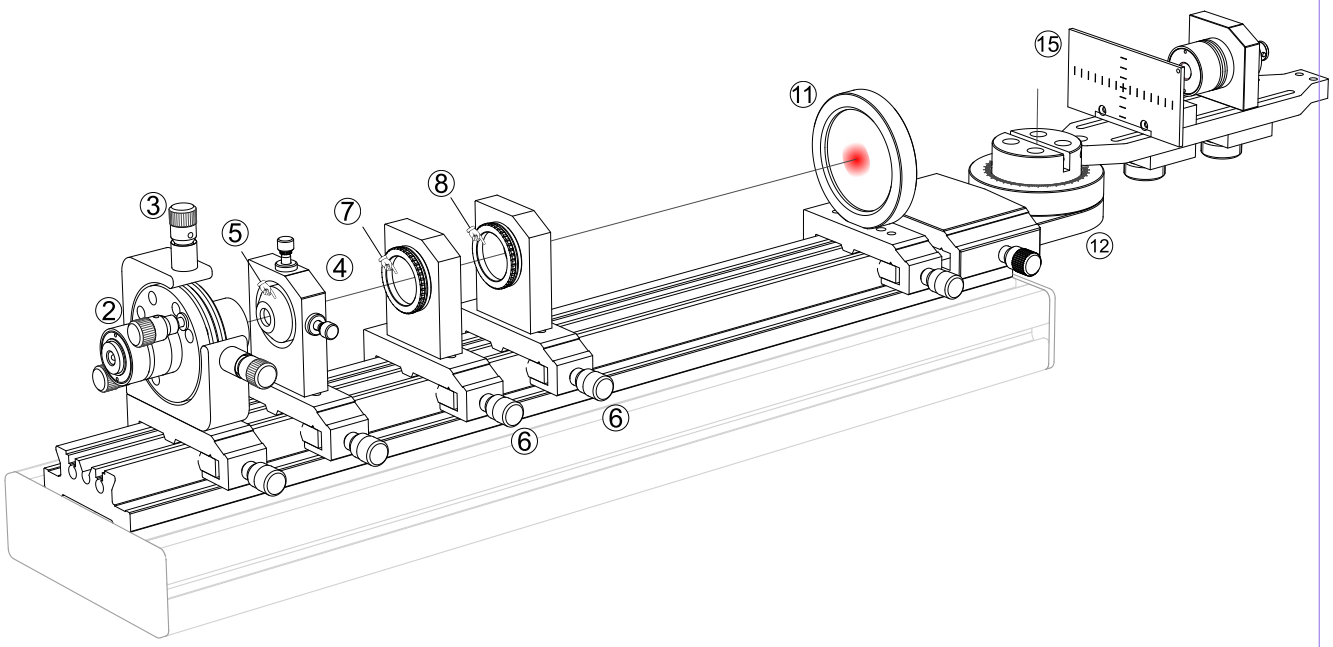

In the next step, we insert the plano-convex cylindrical lens with a focal length of 45 mm (8) behind the plano-concave cylindrical lens (7). Rotating the cylindrical lens changes the beam profile. The best round profile can be found by trial and error. To do this, you also change the distance between the two cylindrical lenses.

3.4 Spectral properties of LED and Laser diode

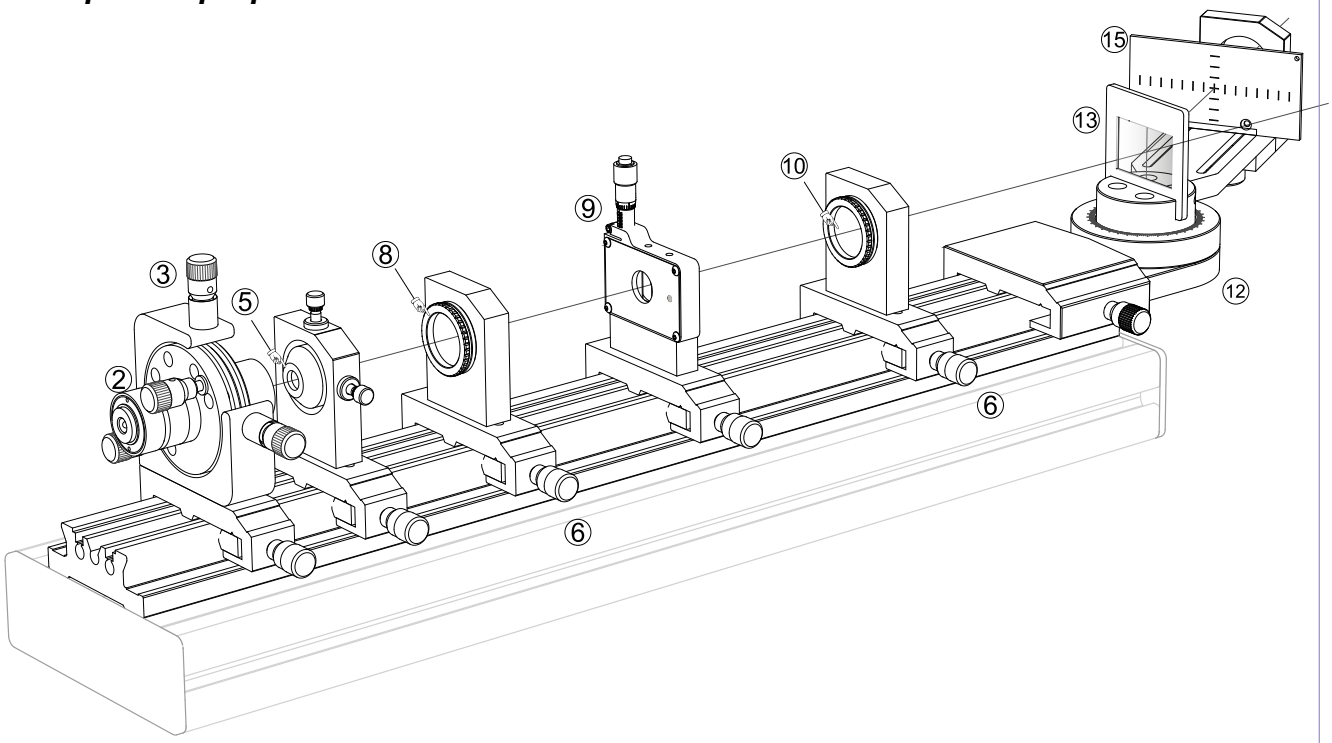

In the following experiment we are interested in the spectral properties of the LEDs and the laser diode. As a spectrometer we use a transmission grating (13) with a line count of 600 lines per millimeter. An adjustable slit ensures a well-resolved line spectrum. In order to obtain strong intensities on the observation screen, we use a cylindrical lens (8) that images as much light as possible onto the slit. The slit image is projected onto the observation screen using an imaging lens (10) with f=40 mm. The cylindrical lens and the imaging lens are moved so that sharp lines are obtained on the screen (15). The zero order with the highest intensity that appears on the screen at zero degrees serves as orientation.

Depending on the distance between the grating and the screen, the first and second order is imaged. Using the equations for the transmission grating and measuring the distances, the wavelength of the light source can be determined.

A particularly beautiful spectrum is produced by the white LED, as it has blue, green and red components.

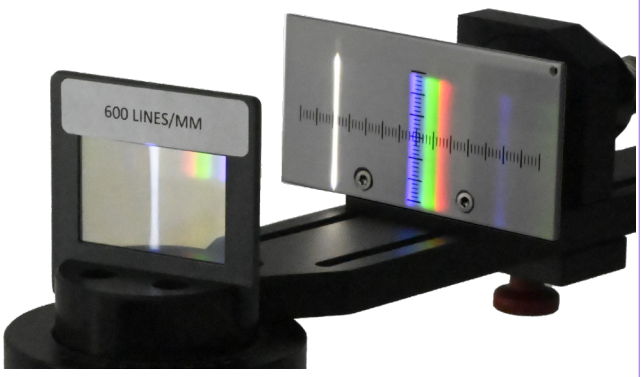

Fig. 27: Spectrum of the white LED